

Wave Propagation Analysis in Inhomogeneous Media by Using the Fourier Method

*Hyun-Sil Kim, *Jae-Seung Kim, *Hyun-Joo Kang, and *Sang-Ryul Kim

*This research was supported by the Ministry of Science and Technology, Republic of Korea.

Abstract

Transient acoustic and elastic wave propagation in inhomogeneous media are studied by using the Fourier method. It is known that the Fourier method has advantages in memory requirements and computing speed over conventional methods such as FDM and FEM, because the Fourier method needs less grid points for achieving the same accuracy. To verify the proposed numerical scheme, several examples having analytic solutions are considered, where two different semi-infinite media are in contact along a plane boundary. The comparisons of numerical results by the Fourier method and analytic solutions show good agreements. In addition, the Fourier method is applied to a layered half-plane, in which an elastic semi-infinite medium is covered by an elastic layer of finite thickness. It is showed how to derive the analytic solutions by using the Cagniard-de Hoop method. The numerical solutions are in excellent agreements with analytic results.

I. Introduction

Wave propagation in inhomogeneous media has been of great importance in various fields such as seismology, ocean acoustics, geophysical problems and electromagnetics. Since analytic solutions are available only on the exceptionally simple problems, most realistic problems of complicated configurations have been studied by using the numerical methods such as the FEM, FDM, and ray tracing technique. The FDM is frequently used to simulate the three-dimensional seismic wave propagation [1], because the algorithm of the FDM is straightforward and suitable for numerical implementations. However, the numerical simulation of earthquakes in real structures by FDM requires a large amount of memories, in which the degrees of freedom often exceeds tens of millions. Recently, the Fourier method (or pseudospectral method) [2,3,4] has gained attentions because it needs relatively small number of grid points for achieving the same accuracy compared to the FDM or FEM. The basic idea of the Fourier method is that the spatial derivatives are computed by the Fourier transform (in practice by the FFT), of which concept has also been used in several applications including vibration [5] and other areas [6]. In FDM, the spatial derivatives are expanded in terms of the finite difference schemes. Fornberg [3] showed that the Fourier method is the limit of the FDM as the order of expansion is increased.

In this paper, we study transient acoustic and elastic

wave propagation in inhomogeneous media by using the Fourier method. The material properties such as density and sound speed are dependent on the position. To verify the numerical schemes, we compare the solution by the Fourier method to the available analytic results. The configuration that two different semi-infinite media are in contact along the plane boundary is the simplest form of the inhomogeneous media, for which analytic solutions are known. As numerical examples, we consider the fluid/fluid, fluid/solid, and solid/solid configurations, where a point force is applied as a source function. In addition, we consider a layered half-plane in which an elastic semi-infinite medium is covered by an elastic layer of uniform thickness, which is one of the fundamental models in seismology. The layered elastic half-plane has served as an important bench mark problem in developing numerical techniques, since it includes free surface and inner reflecting plane. However, no analytic solution was available. In the present study, we show how to derive the analytic solutions of the layer problem and use them as a guide to check the numerical results.

II. Formulations for the Fourier Method

We consider a two-dimensional wave equation in an inhomogeneous media. When density and sound speed of the fluid are functions of the position, the governing equation for acoustic wave is given by

$$\frac{\partial}{\partial x} \left(\frac{1}{\rho} \frac{\partial p}{\partial x} \right) + \frac{\partial}{\partial z} \left(\frac{1}{\rho} \frac{\partial p}{\partial z} \right) + S(x, z, t) = \frac{1}{\rho c^2} \frac{\partial^2 p}{\partial t^2}, \quad (1)$$

* Acoustics Lab. Korea Institute of Machinery and Materials

Manuscript Received : September 24, 1998.

where $\rho(x, z)$ and $c(x, z)$ are density and sound speed, and $S(x, z, t)$ is the source function.

The basic idea of the Fourier method is to use Fourier transform and its properties for computing spatial derivatives. To this end, we define the Fourier transform

$$F(\xi) = \int_{-\infty}^{\infty} e^{-i\xi x} f(x) dx.$$

We recall that the Fourier transform of the derivatives are readily given as

$$(i\xi)^n F(\xi) = \int_{-\infty}^{\infty} e^{-i\xi x} \frac{\partial^n f}{\partial x^n} dx.$$

Since the inhomogeneous medium of interest is infinite (or semi-infinite), we must choose the numerical model to be large enough to contain all the interesting area with sufficient margins. If we consider the derivative, $\partial((1/\rho)\partial p/\partial x)/\partial x$, in Eq. (1), the procedures are as follows:

- (i) First, take the Fourier transform of $p(x, z, t)$ to obtain $P(\xi, z, t)$.
- (ii) Multiply $i\xi$ to P and apply the inverse Fourier transform to compute $\partial p/\partial x$.
- (iii) Multiply $1/\rho$ to $\partial p/\partial x$ and repeat the step (i) and (ii) to get $\partial((1/\rho)\partial p/\partial x)/\partial x$.

The derivative term over z may be treated in a similar way. In practice, we use the Fast Fourier Transform (FFT) to compute the Fourier and inverse Fourier transform. Also, we select the dimension of the model to be 2^n to maximize the efficiency of the FFT program.

We expand the time derivative into the second order finite difference approximation

$$\frac{\partial^2 p}{\partial t^2} = \frac{1}{(\Delta t)^2} (p_{n+1} - 2p_n + p_{n-1}), \quad (2)$$

where Δt is the time increment and p_n is the pressure at $t = n\Delta t$. After rearranging Eqs. (1) and (2), we have

$$p_{n+1} = 2p_n - p_{n-1} + \rho(c\Delta t)^2 \left[\frac{\partial}{\partial x} \left(\frac{1}{\rho} \frac{\partial p_n}{\partial x} \right) + \frac{\partial}{\partial z} \left(\frac{1}{\rho} \frac{\partial p_n}{\partial z} \right) + S(x, z, n\Delta t) \right]. \quad (3)$$

As initial conditions, we assume that there is no movement when $t \leq 0$ (or $p(0) = 0$ and $\partial p(0)/\partial t = 0$), from which we have $p_0 = 0$ and $p_1 = p_{-1}$. When $n = 0$, the spatial derivative terms in Eq. (3) are zero, since FFT computation of p_0 is zero. Then, Eq. (3) becomes

$$p_1 = \frac{\rho(c\Delta t)^2}{2} S(x, z, 0), \quad n = 0.$$

The stability condition [4] requires

$$\frac{c\Delta t}{\Delta d} < \frac{\sqrt{2}}{\pi}, \quad (4)$$

where Δd is the grid size.

Next, we consider the elastic wave propagation in an inhomogeneous medium. The governing equations are given by

$$\rho \frac{\partial^2 u}{\partial t^2} = \frac{\partial \sigma_{xx}}{\partial x} + \frac{\partial \sigma_{xz}}{\partial z} + \rho f_x, \quad (5)$$

$$\rho \frac{\partial^2 w}{\partial t^2} = \frac{\partial \sigma_{xz}}{\partial x} + \frac{\partial \sigma_{zz}}{\partial z} + \rho f_z, \quad (6)$$

where u, w are displacements in x and z directions, and f_x, f_z are body forces. The stresses are related to the displacements as

$$\sigma_{xx} = (\lambda + 2\mu) \frac{\partial u}{\partial x} + \lambda \frac{\partial w}{\partial z}, \quad (7)$$

$$\sigma_{zz} = (\lambda + 2\mu) \frac{\partial w}{\partial z} + \lambda \frac{\partial u}{\partial x}, \quad (8)$$

$$\sigma_{xz} = \mu \left(\frac{\partial u}{\partial z} + \frac{\partial w}{\partial x} \right), \quad (9)$$

where $\lambda(x, z)$ and $\mu(x, z)$ are Lamé coefficients. Eqs. (5)-(9) can be formulated for Fourier method in the same manner as in the acoustic wave equation.

When we model only finite area from an infinite medium for numerical simulation of wave propagation, we always have a problem of artificial reflections at the boundary. The reflected waves re-enter the modeled area and would contaminate the true solution as time increases, which occurs also in FDM and FEM. Several methods have been proposed to eliminate the artificial reflections, among which we employ the method in Ref. [7], because it is simple and suitable for the numerical schemes using regular grids. The basic idea of the method is to introduce the damping zone (or absorbing area) along the boundary of the model, where in the damping zone the amplitude of the wave decreases exponentially.

III. Examples and Comparisons with Analytic Solutions

We apply the Fourier method to the several examples, in which two different semi-infinite media are in contact along a plane boundaries and point source is applied to

the point (x_0, z_0) . In Fig. 1, a typical model for two semi-infinite media in contact is shown, where shaded area represents the damping zone. The analytic solutions for those problems are usually obtained by using the Cagniard-de Hoop method [8].

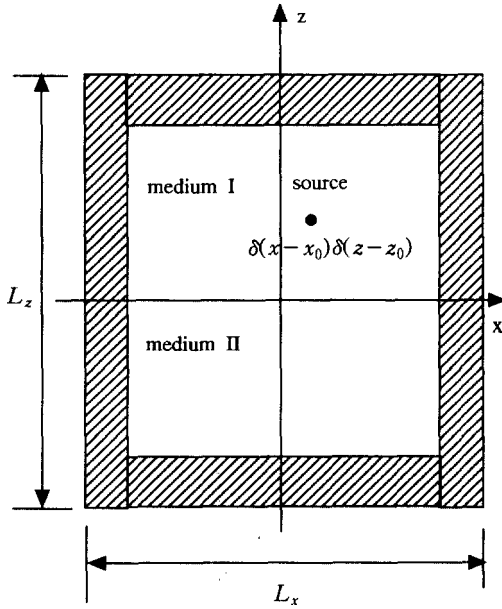


Figure 1. Typical model for two semi-infinite media in contact.

Example 1 : Fluid/Fluid

As the first example, we consider the fluid/fluid configuration, in which a point source is applied in the upper medium

$$z > 0, \quad \frac{\partial^2 p}{\partial x^2} + \frac{\partial^2 p}{\partial z^2} + \delta(x)\delta(z-z_0)f(t) = \frac{1}{c_1^2} \frac{\partial^2 p}{\partial t^2}, \quad (10)$$

$$z < 0, \quad \frac{\partial^2 p}{\partial x^2} + \frac{\partial^2 p}{\partial z^2} = \frac{1}{c_2^2} \frac{\partial^2 p}{\partial t^2}, \quad (11)$$

where c_1 and c_2 are sound speeds of the upper and lower fluid. The boundary conditions at the surface $z=0$ are continuity of pressure and normal component of the velocity

$$p_1 = p_2,$$

$$\frac{1}{\rho_1} \frac{\partial p_1}{\partial z} = \frac{1}{\rho_2} \frac{\partial p_2}{\partial z},$$

where ρ_1 and ρ_2 are density of the upper and lower fluid. The detailed procedures of obtaining solutions of

Eqs. (10) and (11) may be found in the book by Aki and Richards [8].

In numerical examples, we use the nondimensionalized parameters defined as

$$x' = x/L_x, \quad z' = z/L_z, \quad c' = c/c_0, \quad t' = t/(c_0 L_x), \quad \rho' = \rho/\rho_0,$$

where L_x and L_z are the size of the model, and c_0, ρ_0 are reference sound speed and density. We use $c_0 = 1$ m/s and $\rho_0 = 1$ kg/m³. From now on, we drop the prime notation and all parameters are to be understood as nondimensionalized quantities unless units are expressed.

We applied the Fourier method to the area $-0.5 < x, z < 0.5$, and introduced the damping zone along the boundary to absorb the waves. The sound speed and density of the upper and lower fluid are: $\rho_1 = 1.0, c_1 = 1.0; \rho_2 = 1.5, c_2 = 1.2$. The grids are 128×128 and the time increment is 0.001. In numerical simulation of seismogram, the Ricker wavelet is frequently used as a standard source. For a point source, the commonly used source is of the shifted zero phase type given by

$$f(t) = \cos \pi f_0(t-t_0) e^{-0.5 f_0^2(t-t_0)^2}, \quad (12)$$

where f_0 is the cut-off frequency and t_0 is time delay. In this study, we set $f_0 = 50$ Hz and $t_0 = 0.06$ s.

In Fig. 2, we plot the pressure as a function of time at a fixed point at $x=0.125, z=0.25$, while the source position is $x_0=0, z_0=0.125$. The comparison of numerical and analytic response in Fig. 2 shows excellent

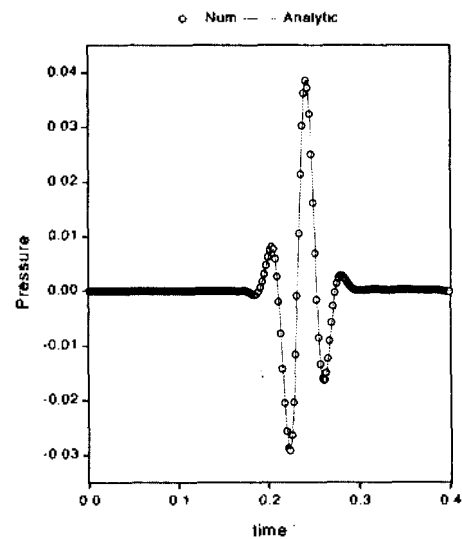


Figure 2. Pressure vs. time at the point $x = 0.125, z = 0.25$.

agreement. In Fig. 3, we plot the snapshot of the pressure at $t = 0.3$. In the upper fluid ($z > 0$), there are two ripples (see Fig. 2 for the cross-section of ripple). The outer ripple corresponds to the direct wave from the source, while inner ripple of relatively smaller amplitude is the reflected wave at the interface $z = 0$. In the lower fluid, there shows one ripple representing transmitted wave. Note that the direct wave looks like a circular arc, whereas reflected wave does not, since the reflection coefficients depends on the incident angle.

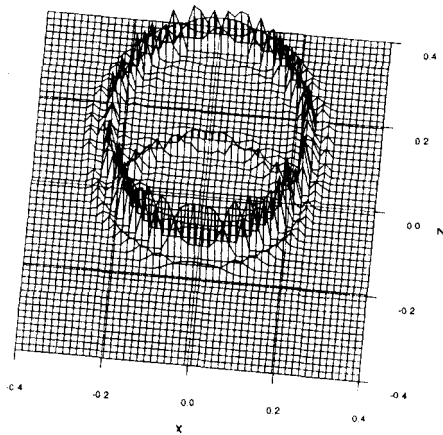


Figure 3. Snapshot of pressure when $t = 0.3$.

Example 2 : Fluid/Solid

The second example is the fluid/solid configuration, of which analytic solution has been obtained by de Hoop and van der Hijden [9,10]. In numerical simulation, we may take the fluid as the special case of the elastic medium. When we set $\mu = 0$ in Eqs. (7)-(9), the stresses σ_{xx} and σ_{zz} become negative pressure, whereas shear stress vanishes

$$\sigma_{xx} = \sigma_{zz} = \lambda \left(\frac{\partial u}{\partial x} + \frac{\partial w}{\partial z} \right) = -p,$$

$$\sigma_{xz} = 0.$$

Eqs. (5) and (6) may be represented as

$$\rho \frac{\partial \vec{v}}{\partial t} = -\nabla p,$$

where \vec{v} is the velocity vector.

We apply the source in the elastic medium at $x_0 = 0$ and $z_0 = -0.125$. In Fig. 4, we plot the pressure for a

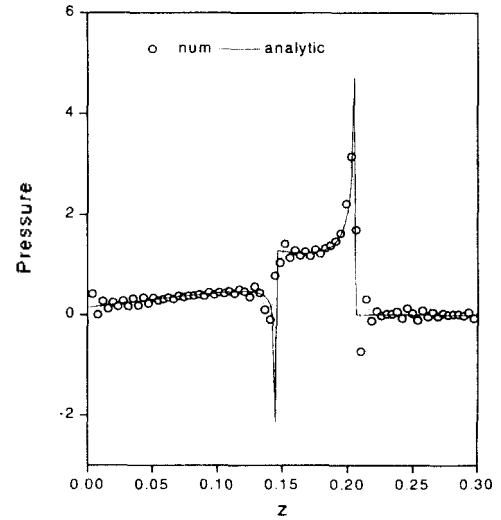


Figure 4. Pressure when $t=0.4$ and source function is $f(t) = H(t)$.

fixed time $t=0.4$ along the line $0 < z < 0.3$ at $x = 0.125$. The density and sound speed of the fluid are $\rho_1 = 1.0$, $c_1 = 0.7$, while the density and sound speed of the P and S wave of the elastic solid are $\rho_2 = 1.5$, $\alpha_2 = 1.5$, $\beta_2 = 0.8$. The grids are 256×256 and the time increment is 0.0005. The source function is $f(t) = H(t)$, where $H(t)$ denotes the Heaviside step function. The comparison in Fig. 4 shows good agreement except the singular points corresponding to the arrival of P and S waves.

Example 3 : Solid/Solid

For the next example, we consider the case of two different elastic media in contact. Although Ben-Menahem and Vered [11] investigated the response of a solid/solid configuration, their concerns were mainly shear dislocations for nonsymmetric sources, and didn't give the solution in a clear and explicit way. Therefore, in the present paper we derive the analytic solutions by using the Cagniard-de Hoop method in the same manner as in the previous examples.

We assume that the point source is applied to the upper medium. After combining Eqs. (5)-(9), the horizontal and vertical displacements u_1 and w_1 of the upper medium are governed by

$$\frac{\partial^2 u_1}{\partial t^2} = \alpha_1^2 \left(\frac{\partial^2 u_1}{\partial x^2} + \frac{\partial^2 w_1}{\partial x \partial z} \right) + \beta_1^2 \left(\frac{\partial^2 u_1}{\partial z^2} - \frac{\partial^2 w_1}{\partial x \partial z} \right) + \delta(x) \delta(z - z_0) f_1(t),$$

$$\frac{\partial^2 w_1}{\partial t^2} = \alpha_1^2 \left(\frac{\partial^2 w_1}{\partial x^2} + \frac{\partial^2 u_1}{\partial x \partial z} \right) + \beta_1^2 \left(\frac{\partial^2 w_1}{\partial z^2} - \frac{\partial^2 u_1}{\partial x \partial z} \right) + \delta(x) \delta(z - z_0) f_s(t), \quad (14)$$

where α_1 and β_1 are sound speeds of P and S waves in the upper medium defined as

$$\alpha_1^2 = (\lambda_1 + 2\mu_1)/\rho_1, \quad \beta_1^2 = \mu_1/\rho_1,$$

and f_x, f_z are time dependent source functions ($z_1 > 0$).

In the lower medium, the displacements are governed by the same equations except that there are no source terms and α_1, β_1 are replaced by α_2, β_2 defined as

$$\alpha_2^2 = (\lambda_2 + 2\mu_2)/\rho_2, \quad \beta_2^2 = \mu_2/\rho_2.$$

After applying the Laplace transform to the time and Fourier transform to x coordinate in Eqs. (13) and (14), we find that the transformed displacements U_1^* and W_1^* of the upper medium satisfy

$$\beta_1^2 \frac{d^2 U_1^*}{dz^2} - (\xi^2 \alpha_1^2 + s^2) U_1^* + i\xi(\alpha_1^2 - \beta_1^2) \frac{dW_1^*}{dz} = -\delta(z - z_0) F_x(s), \quad (15)$$

$$\alpha_1^2 \frac{d^2 W_1^*}{dz^2} - (\xi^2 \beta_1^2 + s^2) W_1^* + i\xi(\alpha_1^2 - \beta_1^2) \frac{dU_1^*}{dz} = -\delta(z - z_0) F_z(s), \quad (16)$$

where ξ, s are the Fourier and Laplace transform variables and F_x, F_z are the Laplace transforms of $f_x(t)$ and $f_z(t)$. Now we change the Fourier transform parameter as $\xi = sq$, which is necessary for applying the Cagniard-de Hoop method in inverting Laplace transform.

The solutions of Eqs. (15) and (16) consist of the particular and complementary solutions. We can obtain the particular solutions after applying the Fourier transform to z coordinate in Eqs. (15) and (16) as if the upper medium were extended infinitely as

$$z < z_0, \quad \begin{pmatrix} U_p^* \\ W_p^* \end{pmatrix} = \begin{pmatrix} q \\ -i\eta_a \end{pmatrix} G_a e^{-\eta_a(z_0 - z)} + \begin{pmatrix} \eta_\beta \\ -iq \end{pmatrix} G_\beta e^{-\eta_\beta(z_0 - z)}, \quad (17)$$

where

$$G_a = \frac{1}{2s} \left(-F_x \frac{q}{\eta_a} + iF_z \right), \quad G_\beta = \frac{1}{2s} \left(F_x - iF_z \frac{q}{\eta_\beta} \right), \\ \eta_a = \sqrt{q^2 + 1/\alpha_1^2}, \quad \eta_\beta = \sqrt{q^2 + 1/\beta_1^2}.$$

When $z > z_0$, similar forms are obtained.

The complementary solutions consist of two terms representing upgoing P and S waves, $e^{-\eta_a z}$ and $e^{-\eta_\beta z}$. Hence, the total solutions of the upper medium are

$$\begin{pmatrix} U_1^* \\ W_1^* \end{pmatrix} = \begin{pmatrix} U_p^* \\ W_p^* \end{pmatrix} + \begin{pmatrix} q \\ i\eta_a \end{pmatrix} A_1 e^{-\eta_a z} + \begin{pmatrix} \eta_\beta \\ iq \end{pmatrix} A_2 e^{-\eta_\beta z}. \quad (18)$$

The transformed displacements U_2^* and W_2^* of the lower medium have only downgoing waves

$$\begin{pmatrix} U_2^* \\ W_2^* \end{pmatrix} = \begin{pmatrix} q \\ -i\gamma_a \end{pmatrix} B_1 e^{\gamma_a z} + \begin{pmatrix} \gamma_\beta \\ -iq \end{pmatrix} B_2 e^{\gamma_\beta z}, \quad (19)$$

where γ_a and γ_β are defined as

$$\gamma_a = \sqrt{q^2 + 1/\alpha_2^2}, \quad \gamma_\beta = \sqrt{q^2 + 1/\beta_2^2}.$$

The four unknowns A_1, A_2 , and B_1, B_2 can be determined from the boundary conditions. At the interface ($z=0$), we need continuity of the displacements and normal and shear stresses

$$u_1 = u_2, \quad w_1 = w_2, \quad (20)$$

$$\sigma_{zz}^1 = \sigma_{zz}^2, \quad \sigma_{zx}^1 = \sigma_{zx}^2. \quad (21)$$

From the boundary conditions, the unknowns are determined as

$$A_1 = r_{PP}^0 G_a e^{-\eta_a z_0} + t_{SP}^0 G_\beta e^{-\eta_\beta z_0}, \quad (22)$$

$$A_2 = r_{PS}^0 G_a e^{-\eta_a z_0} + t_{SS}^0 G_\beta e^{-\eta_\beta z_0}, \quad (23)$$

$$B_1 = t_{PP}^0 G_a e^{-\eta_a z_0} + t_{SP}^0 G_\beta e^{-\eta_\beta z_0}, \quad (24)$$

$$B_2 = t_{PS}^0 G_a e^{-\eta_a z_0} + t_{SS}^0 G_\beta e^{-\eta_\beta z_0}, \quad (25)$$

where r_{PP}^0 means reflection coefficient for P to P wave, and t_{SP}^0 denotes transmission coefficient for S to P wave occurring at $z=0$ (similar meanings hold for other notations). The detailed expressions for reflection and transmission coefficients for two semi-infinite elastic planes in contact may be found in the book by Brekhovskikh and Godin [12]. We may now invert Eqs. (22)-(25) by using the Cagniard-de Hoop techniques (see Ref. [8] for details).

In addition, we consider a layered half-plane where an elastic semi-infinite medium is covered by an elastic layer of uniform thickness and a point source acts in the layer as shown in Fig. 5. The earlier works [13] have been concentrated on the dispersion curves. The procedures

of deriving the analytic solutions are basically the same as in the case of two semi-infinite elastic media in contact. However, two additional terms arise in Eq. (18) in the finite layer, since upper bound at $z=H$ causes reflections. As waves are confined in the layer of finite thickness, there are numerous reflections and transmissions so that the final forms consist of the infinite series. We are preparing the analytic solutions in a separate paper [14].

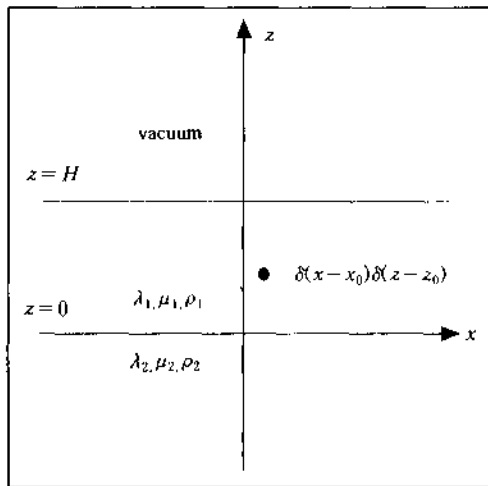


Figure 5. Layered elastic half-plane.

For numerical examples, we consider the following material properties:

Upper medium : $\alpha_1 = 1.0, \beta_1 = 1.0, \rho_1 = 1.0$
 Lower medium : $\alpha_2 = 1.5, \beta_2 = 0.8, \rho_2 = 1.5$

The height of the layer is $H=0.2$ and source and receiver positions are $x_0 = 0, z_0 = 0.125, x = z = 0.0938$. We assume that time dependence of the source is given by

$$f_x = f_z = H(t).$$

In numerical modeling for the case of the layer, the region ($z > H$) over the layer has zero Lamé constants to simulate the stress-free conditions. The grids are 128×128 and the time increment is 0.001.

In Fig. 6, we compared the numerical results (symbols) with analytic ones (solid and dotted lines) for two cases ($H=0.2$ and $H=\infty$), which show good agreements. We find that two results for $H=0.2$ and $H=\infty$ are in perfect agreements until the first reflection of the

P wave at $z=H$ when $t=0.204$.

As the last example, we study a more complicated model as shown in Fig. 7. The material properties are:

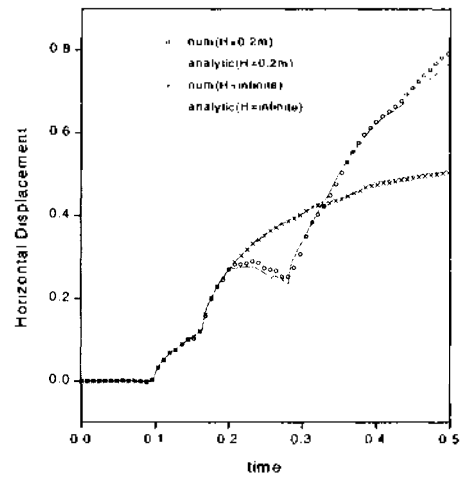


Figure 6. Comparisons of horizontal displacements when the thickness of the layer is finite and infinite.

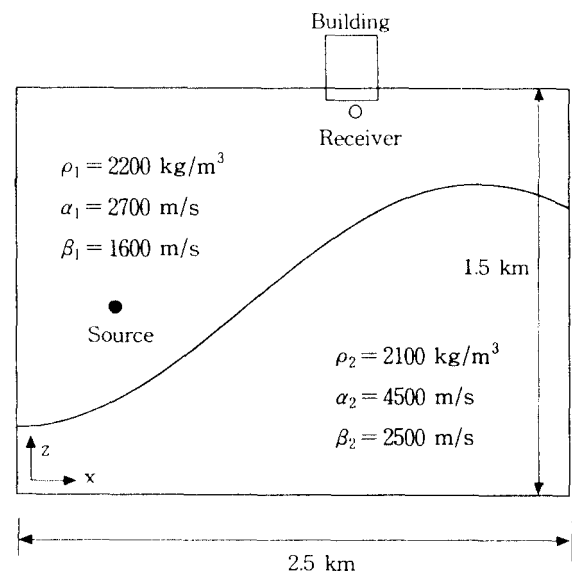


Figure 7. Model for continuously varying surface. The source and receiver positions are; $x_0 = 0.5 \text{ km}, z_0 = 0.7 \text{ km}$, and $x = 1.5 \text{ km}, z = 1.45 \text{ km}$.

Upper medium : $\alpha_1 = 2700 \text{ m/s}, \beta_1 = 1600 \text{ m/s}, \rho_1 = 2200 \text{ kg/m}^3$

Lower medium : $\alpha_2 = 4500 \text{ m/s}, \beta_2 = 2500 \text{ m/s}, \rho_2 = 2100 \text{ kg/m}^3$

The size of the area is $2.5 \text{ km} \times 1.5 \text{ km}$, and we added zero paddings over the region $1.5 \text{ km} < z < 2.5 \text{ km}$ for

simulating vacuum area over the surface. In this model, the length, sound speed and density are nondimensionalized with respect to $L_x (= 2.5 \text{ km})$, α_2 and ρ_2 . We used 128×128 grids so that the grid size is 23.4 m . The source and receiver positions are: $x = 0.5 \text{ km}$, $z = 0.7 \text{ km}$ for source, and $x = 1.5 \text{ km}$, $z = 1.45 \text{ km}$ for receiver (the receiver position is below the hypothetical building). We also used the source function defined in Eq. (12). In Fig. 8, we plot the stresses at the receiving point as a function of the time, which may be used as input functions for another applications such as seismic analysis of the building. In Fig. 8, the stresses and time are nondimensionalized with respect to $\rho_2 \alpha_2^2$ and L_x / α_2 .

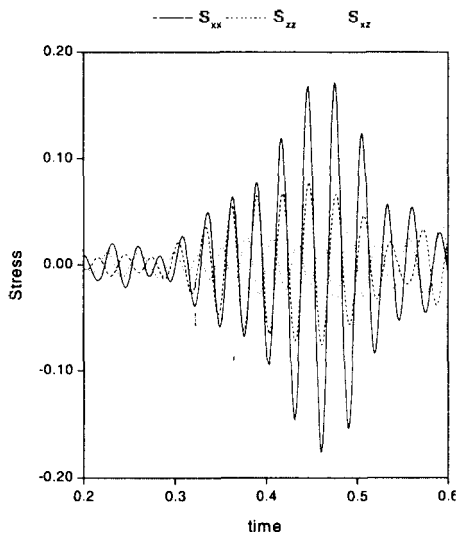


Figure 8. Stresses vs. time at the receiver position.

IV. Conclusions

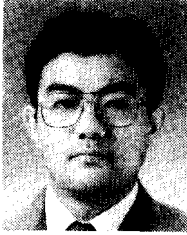
In this paper, we have studied transient acoustic and elastic wave propagation in inhomogeneous media by using the Fourier method. The Fourier method has advantages in memory requirements and computing speed over conventional methods such as FDM and FEM, because the Fourier method needs less grid points for achieving the same accuracy. As numerical examples, we considered the fluid/fluid, fluid/solid, and solid/solid configurations, where two different semi-infinite media are in contact along a plane boundary and analytic solutions are available. In numerical model, we introduced the damping zone along the boundary to eliminate the artificially reflecting waves at the boundary. In addition, we studied a layered half-plane, in which an elastic semi-infinite medium is covered by an elastic layer of uniform thickness. The

layered elastic half-plane is one of the basic models in seismology, but no exact solution is known. We showed how to derive the analytic solutions by using the Cagniard method. The comparisons of numerical and analytic solutions all showed good agreements. Although only two-dimensional problems are treated in the present study, the Fourier method can readily be applied to the three-dimensional wave problems.

References

1. A. Frankel and J. Vidale, "A three-dimensional simulation of seismic waves in the Santa Clara Valley, California, from a Loma Prieta Aftershock," *Bulletin of the Seismological Society of America*, Vol. 82, No. 5, pp. 2045-2074, October 1992.
2. M. Reshef, D. Kosloff, M. Edwards, and C. Hsiung, "Three-dimensional elastic modeling by the Fourier method," *Geophysics*, Vol. 53, No. 9, pp. 1184-1193, September, 1988.
3. B. Fornberg, "The pseudospectral method: comparisons with finite differences for the elastic wave equation," *Geophysics*, Vol. 52, No. 4, pp. 483-501, April, 1988.
4. D. D. Kosloff and E. Baysal, "Forward modeling by a Fourier method," *Geophysics*, Vol. 47, No. 10, pp. 1402-1412, October, 1982.
5. J. F. Doyle, *Wave Propagation in Structures*, Springer-Verlag, New York, 1989.
6. D. Gorlicb and S. A. Orszag, *Numerical Analysis of Spectral Methods: Theory and Applications*, SIAM Monograph, 1977.
7. C. Cerjan, D. Kosloff, R. Kosloff, and M. Reshef, "A non-reflecting boundary condition for discrete acoustic and elastic wave equations," *Geophysics*, Vol. 50, No. 4, pp. 705-708, 1985.
8. K. Aki and P. G. Richards, *Quantitative Seismology, Theory and Methods*, Freeman, San Francisco, 1980.
9. A. T. de Hoop and J. H. van der Hijden, "Generation of acoustic waves by an impulsive line source in a fluid/solid configuration with a plane boundary," *The Journal of the Acoustical Society of America*, Vol. 74, pp. 333-342, 1983.
10. A. T. de Hoop and J. H. van der Hijden, "Generation of acoustic waves by an impulsive point source in a fluid/solid configuration with a plane boundary," *The Journal of the Acoustical Society of America*, Vol. 75, pp. 1709-1715, 1984.
11. A. Ben-Menahem and M. Vered, "Extension and interpretation of the Cagniard-Pekeris method for dislocation sources," *Bulletin of the Seismological Society of America*, Vol. 63, pp. 1611-1636, 1973.
12. L. M. Brekhovskikh and O. A. Godin, *Acoustics of Layered Media I*, Springer-Verlag, Heidelberg, 1990.
13. W. M. Ewing, W. S. Jardetzky, and F. Press, *Elastic Waves in Layered Media*, McGraw-Hill, New York, 1957.
14. Hyun-Sil Kim, Jae-Seung Kim, Hyun-Joo Kang, and Sang-Ryul Kim, "Transient wave propagation in a multilayered elastic half-plane," submitted to the *Journal of the Acoustical Society of America*, 1998.

▲Hyun-Sil Kim



Hyun-Sil Kim he received a B.S. degree in ME(mechanical engineering) from Seoul National University in 1980, and a M.S. degree in ME from KAIST in 1982. He received a Ph.D. degree in ME(major on nonlinear acoustics) from GIT in 1989. His research interests includes numerical simulation of acoustic and elastic wave propagation, power flow, and architectural acoustics.

▲Jae-Seung Kim



Jae-Seung Kim he received B.S. and M.S. degree in naval architectural engineering from Seoul National University in 1976 and 1980, and a Ph.D. degree in ocean engineering from MIT in 1984. He is the head of the acoustics laboratory and his research interests are in structural acoustics, flow noise, and SEA.

▲Hyun-Joo Kang



Hyun-Joo Kang he received a B.S. degree in naval architectural engineering from Cheju National University in 1984, and a M.S. degree in naval architectural engineering from Pusan National University in 1986. His research fields includes sound transmission in panels, structural acoustics, and SEA.

▲Sang-Ryul Kim



Sang-Ryul Kim he received a B.S. degree in ME from Pusan National University in 1993, and a M.S. degree in ME from KAIST in 1995. He is interested in structural acoustics, flow noise, and acoustical measurements.